Edelweiss Applied Science and Technology
ISSN: 2576-8484
Vol. 9, No. 5, 2965-2979
2025
Publisher: Learning Gate
DOI: 10.55214/25768484.v9i5.7626

Study of flow and heat transfer in combination of curved and straight tubes in square arrangement at a subcritical Reynolds number of 35000

Kunal[1*], Sushil Kumar Dhiman[2]
[1,2]Department of Mechanical Engineering, Birla Institute of Technology, Mesra, India, 835215; kunalkumar71@yahoo.in (K.) skdhiman@bitmesra.ac.in (S.K.D.).

Abstract: Numerical analysis of flow dynamics and heat transfer from the external surface of four cylinders in a square arrangement has been conducted in this study. The combination of curved and straight tubes, which finds application in waste heat recovery recuperators, has been investigated. The curved tubes have been placed in upstream positions in concave and convex configurations. All the tubes are subjected to a constant heat flux condition. The study has been carried out at a subcritical Reynolds number of 35,000. The spacing ratio between the cylinders has been varied from 1.5 to 4.0, and the curvature ratio has been varied from 0.5 to 1.5. Local and overall heat transfer and pressure at different heights and at different angular distances have been investigated. The computations have been conducted in commercial Ansys Fluent software using the k-kl-ω turbulence model. The heat transfer, in general, is found to increase when a combination of curved and straight tubes is used instead of a conventional straight tube combination. Maximum heat transfer enhancement is found in CX-ST CR 1.5 SR 1.5. In terms of heat transfer ratio, CX-ST CR 1.5 SR 3.0 is the most efficient, with a 65.43% increase in heat transfer.

Keywords: *Computational fluid dynamics, Convective heat transfer, Cross-flow, tube banks, Curvature ratio, Curved tubes, Spacing ratio.*

1. Introduction

Heat transfer from tube banks is a widely used configuration in industries [1-3]. Cross-flow of air is generally employed in such tube banks [4, 5]. Conventionally, straight circular tubes are used in these tube banks and it finds application in marine engineering, circuits, chemical industry and other related industries. A particular application of tube bank is in waste heat recovery recuperators which utilises straight tube bundle [6-9]. However, the use of combination of curved and straight tube bundle has increased in recent times. In such recuperators the flow passes from a curved tube which is kept either in concave and convex configuration followed by a straight tube. These curved tubes alter the flow and heat transfer. This alteration in flow and heat transfer may be desired and may be manipulated to our advantage by increasing the heat transfer compared to the conventional straight tubes [10].

Heat transfer enhancement techniques from tube bundles is generally classified into three categories namely: Active, passive and mixed. Active methods employ those methods which require external power, passive methods do not require external power rather rely on modification such as change in shape, addition of fins, altering roughness etc. [11, 12]. Mixed method involves the use of both active as well as passive methods. The flow and heat transfer behaviour of a cylinder in tube bank is different from that of an isolated tube [13]. Shear layer interaction and wake interaction takes place in tube bundle when tubes are placed in proximity to other tubes. It further depends on factors such as turbulence intensity, arrangement of tube, Reynolds number (Re), rheological property of fluid, shape of tube Morenko and Fedyaev [14]; Xiao and Zhang [15]; Patil, et al. [16]; Benmansour and Laidoudi [17] and Zafar and Alam [18]. Hishikar, et al. [19] studied the heat transfer in four tube arrangement

History: Received: 24 March 2025; Revised: 16 May 2025; Accepted: 19 May 2025; Published: 28 May 2025
* Correspondence: kunalkumar71@yahoo.in

and found that the flow structure, pressure distribution and heat transfer is strong function of spacing ratio between the tubes. Žukauskas [13] and Khan, et al. [20] developed mathematical equation that correlated the different flow parameters such as Reynolds number, Prandtl number with Nusselt number to predict the heat transfer in tube banks. Aydin, et al. [21] found that heat transfer increases with increase in blockage as well as spacing ratio on the upstream cylinder in tandem arrangement of tubes. Igarashi [22, 23] found different shedding regimes with varying spacing ratio between the tandem tubes. Hu, et al. [24] performed simulations on two tandem cylinders and found that for spacing ratio, SR<3.5, vortex street was found only behind downstream tube and for SR≥3.5, the shear layer from upstream cylinder rolls up before the downstream tube and shedding occurs from both the tube. Investigation by Wang, et al. [25] show three different flow regimes for inline square arrangement of tube. These regimes were classified as shielding regime (SR≤2.0), reattachment regime (2.5≤SR≤3.5) and impinging regime (SR≥4.0). Different turbulence models are often employed by researchers [19, 26-28]. Turbulence models such as LES and DNS require large computational resource however, models such as transition k-kl-ω are suitable for subcritical flows. Hosseini, et al. [29] found that temperature gradient were transported by the vortex shedding. Curved tubes [30, 31] have different flow structures compared to the straight tube. Also, the heat transfer in curved tube is significantly different from the straight tubes. Ring shaped curved tube with vertical and extensions are often used and it has been found that the boundary layer on the horizontal or vertical extension is either thinner or thicker and hence velocity profile is different than the straight tubes [32]. The shedding frequency is different in case of curved tube at different heights [33, 34].

Although the combination of curved tube and straight tube is widely used in the waste hear recovery systems, its thermal performance under unsteady conditions has not been analysed. Three different types of tube bundles with straight tubes and combination of curved (concave and convex) and straight tube is used in waste recovery recuperators have been shown in Fig.1. The present work analyses the heat transfer in four tube arrays with curved tube placed in upstream position and straight tubes in the downstream position. External surfaces of tubes are given a uniform heat flux condition at Re=35000. The effect of curvature ratio, CR of curved tubes and spacing ratio, SR between the tubes in cross-flow of air has been analysed. The results obtained for combination of tubes has been compared with conventional straight tube. Numerical simulations were performed in Ansys-fluent software and k-kl-ω turbulence model was used to predict the flow and heat transfer in the present study.

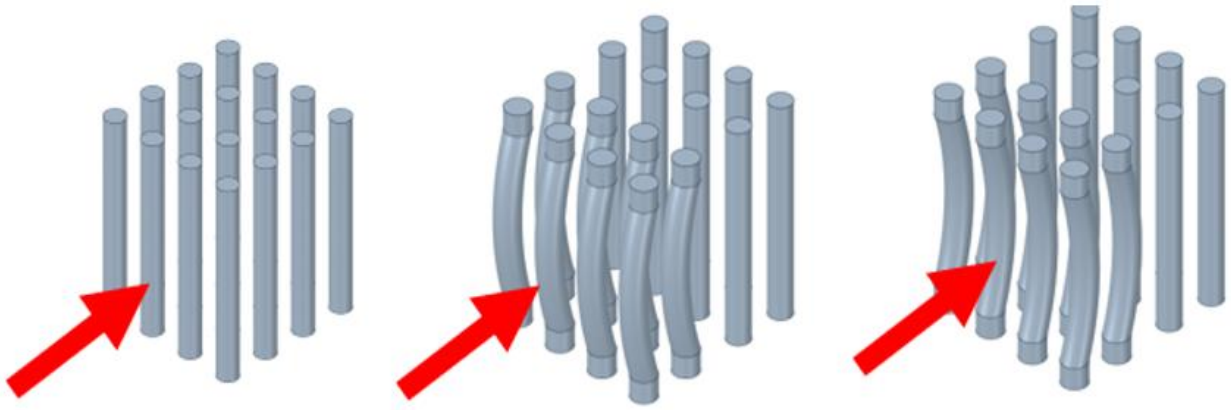

Figure 1.
Different types of tube bundles used in waste heat recovery recuperators (Red arrows denote the flow direction).

Edelweiss Applied Science and Technology
ISSN: 2576-8484
Vol. 9, No. 5: 2965-2979, 2025
DOI: 10.55214/25768484.v9i5.7626

Nomenclature.

CV	Concave tube	C_L	Lift coefficient
CX	Convex tube	C_D	Drag coefficient
ST	Straight Tube	St	Strouhal number
CT	Curved Tube	Nu	Nusselt number
D	Outer Diameter of tube	Nu_{avg}	Average Nusselt number
L	Inter-tube spacing from center of one tube to another	C_p	Coefficient of pressure
C	Deflection of the tube at the central location	θ	Angular position on the tube surface (in degree)
CR	Curvature ratio = C/D	f	Vortex shedding frequency
SR	Spacing Ratio =L/D	ρ	Density
U_∞	Mainstream velocity	k	Thermal conductivity coefficient of tube
ν	Kinematic viscosity	h	Convective heat transfer coefficient
HTR	Heat transfer Ratio	Re	Reynolds number = $\rho U_\infty/\nu$
ST-ST	Straight tubes are placed in upstream as well as downstream positions	CV-ST	Concave tubes are placed in upstream position and straight tube in downstream position
CT-ST	Curved tubes are placed in upstream position and straight tube in downstream position	CX-ST	Convex tubes are placed in upstream position and straight tube in downstream position

2. Numerical Scheme

Present computation is 3-dimensional and involves transient study. Continuity, momentum and energy equations as shown below has been solved by the fluent solver. Beside these equations, turbulence model equations of k-kl-ω given by Walters and Cokljat [35] have been solved. Pressure solver was used to solve the computation. The inlet and outlet of the domain were given velocity inlet and pressure outflow boundary condition. All the other outer cuboidal surfaces (top, bottom, front and rear) were given symmetry boundary condition. The tube surfaces were given a constant heat flux condition with no-slip condition. SIMPLEC pressure-velocity coupling was chosen and spatial discretization of gradient was least square cell based. Pressure, momentum, kinetic energy and energy were solved using second order upwind. Time step of 10^{-4} was given with 20 iteration per time step. Solution was initialised using hybrid initialisation.

Continuity equation:

$$\frac{\partial \rho}{\partial \tau} + \nabla\left(\rho \overline{V}\right) = 0$$

N-S equation:

$$\frac{D\overline{V}}{D\tau} = \frac{-1}{\rho}\nabla p + v\nabla^2\overline{V}$$

which is modified as

Edelweiss Applied Science and Technology
ISSN: 2576-8484
Vol. 9, No. 5: 2965-2979, 2025
DOI: 10.55214/25768484.v9i5.7626

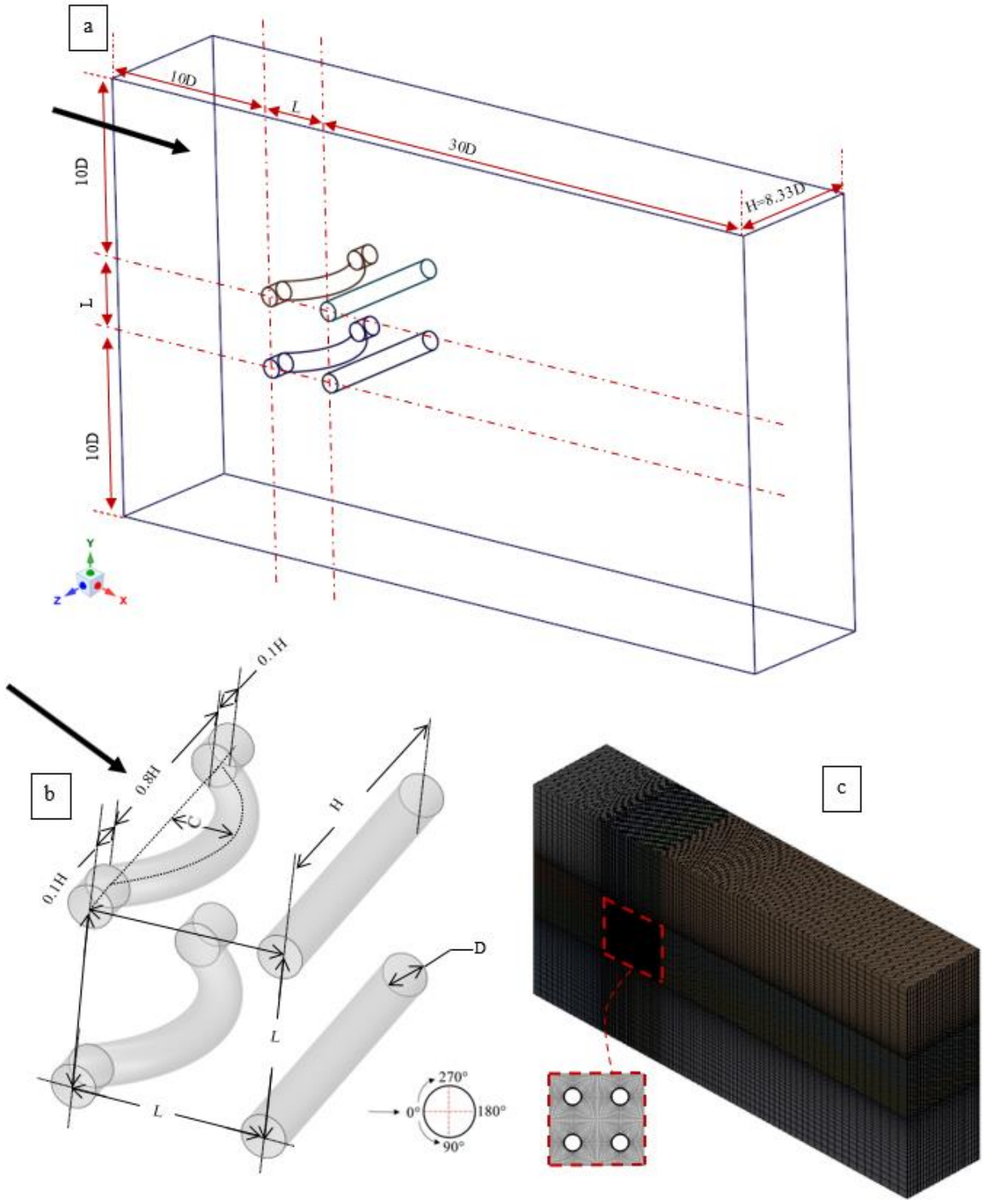

Figure 2.
a).3-D domain of the model with dimensions and flow direction shown in black arrow b) Dimensions of the tube c) 3-D structured mesh prepared in Ansys Workbench

Edelweiss Applied Science and Technology
ISSN: 2576-8484
Vol. 9, No. 5: 2965-2979, 2025
DOI: 10.55214/25768484.v9i5.7626

$$\frac{D\overline{V}}{D\tau} = \frac{-1}{\rho}\nabla p + \nabla\left[\overline{V}\left(\nabla\overline{V} - \overline{u_m u_n}\right)\right]$$

where $-\overline{u_m u_n}$ is the turbulent stress term represented by Boussinesq equation. For instance for the x-momentum equation turbulent stress terms is represented as $-\overline{u_i u_j} = \nu_{tot}\left(\frac{\partial V_i}{\partial y} + \frac{\partial V_j}{\partial x}\right) - \frac{2}{3}k_{tot}\delta_{i,j}$, where ν_{tot} is total kinematic eddy viscosity and k_{tot} is the total turbulent kinetic energy. Note that the k_{tot} considers laminar energies and large scale as well as small scale turbulent energies.
In the equation, m or n represents i or j or k based on matched or unmatched derivative terms with the direction of equation, however, for the matched derivative terms with the direction of equation m=n for which $-\overline{u_m u_n} = 0$

Energy equation:

$$\frac{De}{D\tau} = \alpha c_p \nabla^2 T, where\ e = \overline{V}\nabla\left(c_p T\right)c$$

In terms of T this may be modified as:

$$\frac{DT}{D\tau} = \nabla\left(\alpha\nabla T - \overline{u_m\zeta}\right)$$

where $-\overline{u_m\zeta}$ is the Fourier's relation, for instance for $m = i$, $-\overline{u_m\zeta} = \alpha_{\zeta,tot}\left({}^{\partial T}/_{\partial x_i}\right)$ and $-\overline{u_m\zeta} = 0$ for the y and z derivatives. The equations consider ζ_{tot} represents temperature fluctuations and $\alpha_{\zeta,tot}$ total thermal diffusivity

3. Domain, Geometry Details and Terms Representation

The model has been designed in Ansys workbench. The domain is cuboidal shaped with tubes placed inside it as shown in the Fig.2a. The details of the dimensions of domain and tubes have been mentioned in the Fig.2b. All tubes have a circular cross section having outer diameter, D=30mm. The freestream velocity is 17.04m/s which gives the Re=35000 based on the outer diameter. The total length, H of all the tubes is 250mm. Curved tubes have straight portion at both the ends as shown. The curved tubes are once kept as concave and once as convex. The curvature ratio, (CR=C/D) for the curved tube is defined as the central deflection, C to the diameter, D of the tube. Three different CR=0.5,1.0 and1.5 have been studied in the present work. The spacing ratio, (SR=L/D) is the centre-to-centre distance between the tubes to the diameter of the tube as shown in Fig.2b. It has been varied from 1.5 to 4.0 in the incremental order of 0.5. The curved tube which is either concave or convex is denoted by CT. The concave, convex and straight tubes has been denoted with CV, CX And ST respectively and the square array arrangement having concave in upstream and straight in downstream position is denoted as CV-ST. Similarly, CX-ST is used for convex-straight combinations. Some of the combination of CV-ST combinations are not possible since the projection of the CV tube is towards the downstream tube and it starts making contact with straight tube surface below certain SR. The pressure and Nusselt number distribution in the tubes has been studied at six different non-dimensional heights of tube (z/H=0,0.1,0.2,0.3,0.4 and 0.5). Here, z/H=0, 0.1 and 0.5 corresponds to base of the tube, junction of straight-curved portion in curved tubes and mid-length of the tube.

4. Grid Independence and Validation

Simulations were performed in Ansys-fluent software. Grid independence test was performed for 9 different mesh with various parameters varied. Based on the simulation results it was found that the grid with Case(iii) having 504840 cell counts gave the best results and further refinement of the mesh did not yield significant changes in the result. The mesh for all the models were prepared on the similar pattern. The grid independence test result has been shown in Table1. The comparison of the Nusselt number with Igarashi [22] and Tsutsui and Igarashi [36] has been shown in the Figure 3(a&b). The

Edelweiss Applied Science and Technology
ISSN: 2576-8484
Vol. 9, No. 5: 2965-2979, 2025
DOI: 10.55214/25768484.v9i5.7626

findings of the current work are in considerable agreement with the previously published literatures. Comparison of results from literature have been shown in the Table 2.

Table 1.
Various grid sizes and time steps for grid independence test.

Sl. No.	Times step size($x10^{-4}$)	Minimum cell distance($x10^{-5}$) (in mm)	Number of Cell	C_L	C_D	Nu_{avg}
i.	1	1.3	322290	± 1.19	1.16	140.0
ii.	1	1.3	403648	± 1.40	1.35	162.77
iii.	**1**	**1.3**	**504840**	**± 1.48**	**1.39**	**162.50**
iv.	1	1.3	631040	± 1.48	1.39	162.10
v.	5	1.3	631040	±1.18	1.48	142.21
vi.	5	6.5	794848	± 1.6	1.45	139.43
vii.	1	1.3	403648	± 1.52	1.75	170.56
viii.	1	1.3	503678	± 1.75	1.75	154.32
ix.	1	6.5	503678	± 1.75	1.45	178.12

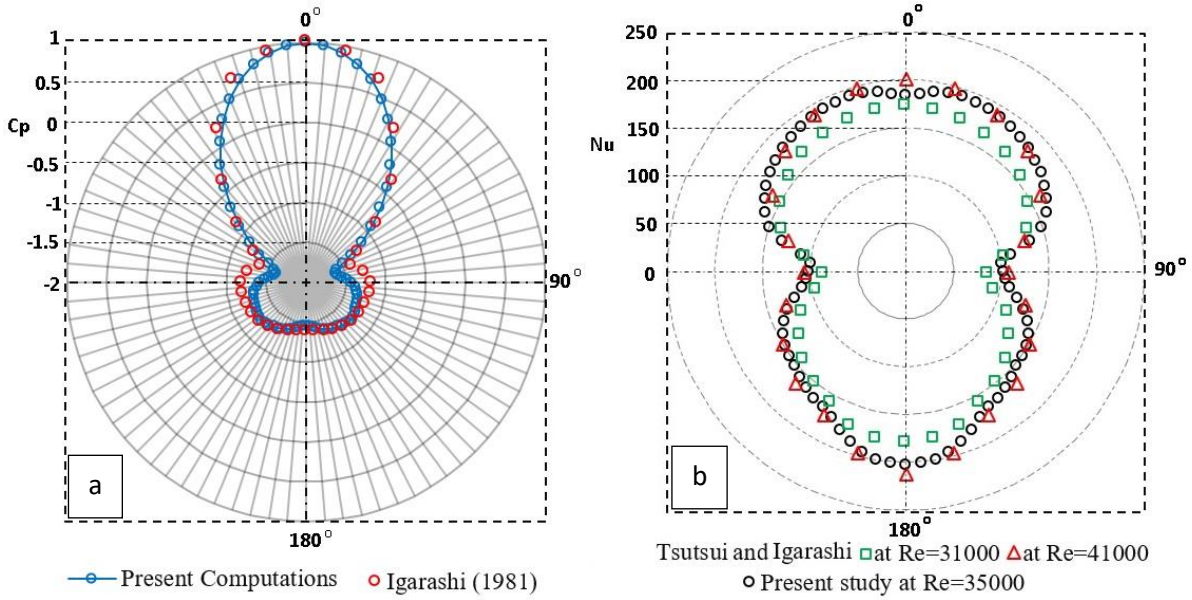

Figure 3.
(a) Comparison of time averaged C_p distribution around tube at the central plane at Re=35000 with Igarashi [22] (b) Comparison of time averaged Nu distribution around tube at the central plane at Re=35000 from present computations, at Re = 31000 and Re = 41000 from Tsutsui and Igarashi [36].

Table 2.
Comparison of the present computational result with the previously published literatures.

Sl.No.	Author	C_D	C_L	$St = fD/U_\infty$	$Nu_{avg.}$
i.	Holfeld [9]	1.30	-	0.20	-
ii.	Hishikar, et al. [19]	1.38	±1.45	0.18	156
iii.	Dhiman, et al. [28]	1.34	±1.36	0.18	154
iv.	Perkins Jr and Leppert [37]	-	-	-	156
v.	Hover, et al. [38]	1.38	±1.16	0.18	-
vi.	Alam, et al. [39]	1.12	±0.96	0.19	-
vii.	Bakkhoshnevis, et al. [40]	1.30	-	0.19	-
viii.	Present Study	1.48	±1.39	0.178	162.50

Edelweiss Applied Science and Technology
ISSN: 2576-8484
Vol. 9, No. 5: 2965-2979, 2025
DOI: 10.55214/25768484.v9i5.7626

5. Results and Discussion

In order to analyse the thermo-fluid characteristics of the combination of straight and curved tube several parameters such as pressure of coefficient, Nusselt number distribution, vorticity core contours and heat transfer ratio has been discussed in the upcoming sections. These parameters address the reason for enhanced heat transfer in case of combination tubes compared to convention ST-ST tubes.

5.1. Heat Transfer

Area weighted average of Nusselt number, ($Nu_{avg}=\bar{h}D/k$) of the whole array of four tubes for different configurations has been presented in the Table3. In ST-ST tube array maximum heat transfer takes place in SR=1.5. The heat transfer in ST-ST combinations decrease from SR 1.5 to 3.0 then start to increase. This may be due to change in flow regime at higher SR. Similarly, maximum heat transfer in CV-ST and CX-ST combinations is takes place in CV-ST CR 0.5 SR 2.0 and CX-ST CR 1.5 SR 1.5 respectively. The heat transfer in CT-ST tube is generally higher than the conventional ST-ST tube combination for same SR. All the 12 possible combinations of CV-ST combinations have higher heat transfer compared to ST-ST counterpart with same SR. In case of CX-ST, 16 out of 18 combinations has higher Nusselt number compared to ST-ST counterpart with same SR. In general, for the same SR, the Nu_{avg} increases with increase in CR in CT-ST combinations. Minimum heat transfer in ST-ST, CV-ST and CX-ST combinations takes place in SR 2.5, CR 0.5 SR 4.0 and CR 0.5 SR 1.5 respectively. The Local pressure distribution and local Nusselt number distribution over the tube combinations having maximum heat transfer have been discussed in the subsequent sections.

Table 3.
Averaged Nusselt number, Nu_{avg} on the array of tubes of different combinations.

SR	ST-ST	CV-ST			CX-ST		
		CR 0.5	CR 1.0	CR 1.5	CR 0.5	CR 1.0	CR 1.5
1.5	166.25	----------	----------	----------	141.80	148.34	188.13
2.0	135.61	184.44	----------	----------	149.56	154.62	154.32
2.5	135.32	182.92	181.00	----------	149.56	155.89	163.37
3.0	111.68	170.39	179.12	165.55	147.88	184.73	184.77
3.5	137.64	155.51	161.69	163.22	147.10	166.95	183.58
4.0	138.23	150.68	158.84	159.79	145.83	149.98	154.58

5.2. Local Nusselt Number

Since the tubes are arranged in square arrangement, therefore, both upstream tubes have same Local Pressure and local heat transfer distribution.

Edelweiss Applied Science and Technology
ISSN: 2576-8484
Vol. 9, No. 5: 2965-2979, 2025
DOI: 10.55214/25768484.v9i5.7626

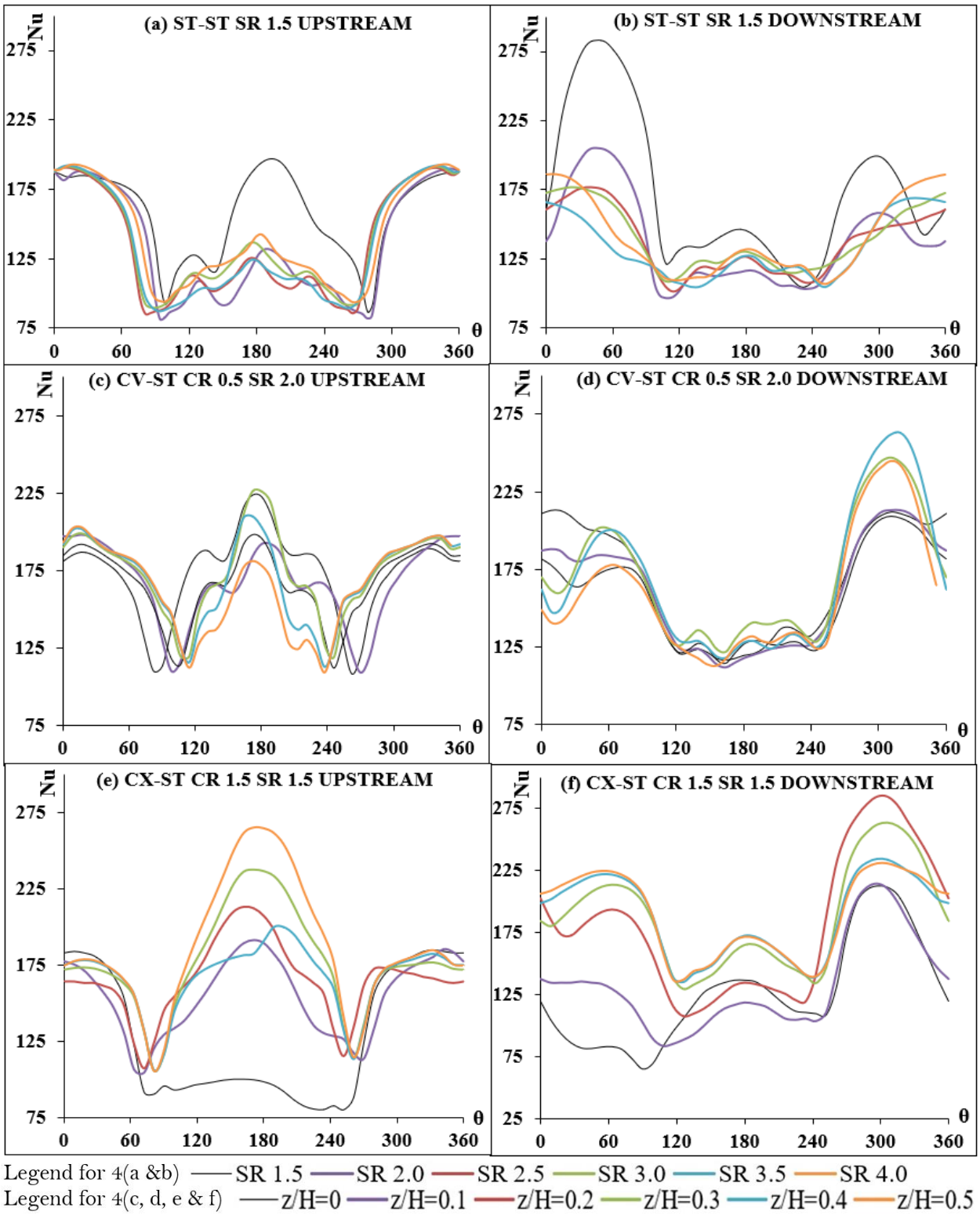

Figure 4.
Local Nusselt Number distribution over the surface of the tube at different SR and CR.

Edelweiss Applied Science and Technology
ISSN: 2576-8484
Vol. 9, No. 5: 2965-2979, 2025
DOI: 10.55214/25768484.v9i5.7626

It is for this reason that both these parameters on only one upstream tube have been studied. Similarly, one tube in downstream has been studied.

Figure 3(a&b) shows Nusselt number distribution on a ST-ST combination in the upstream and downstream position for different SR. In Fig.3a the Nu-distribution shows that the heat transfer decreases from the frontal portion of the tube and then forms a minima in the range of (80-100)° and (265-280)°. This happens because of the boundary layer growth upto these range of angular positions. The heat transfer increases after the laminar shear layer separation and then again decreases slightly which indicates a turbulent shear layer separation zone which lies in the region around (140-150) ° and (205-210)° and then rises upto the rear stagnation point. In all the cases except SR=1 .5, the maximum heat transfer is taking place from the frontal portion at around (0 to 90) ° and (270 to 360) ° of the tube. Amongst all the configurations of the straight tube studied, the maximum heat transfer is taking place in the SR=1.5. Fig.3b shows the heat transfer from the tube in ST-ST combination in the downstream position. There is hump formation due to local maxima formation at around 45° and 300° in the lower SR which vanishes in higher SR. This happens because the separated shear layer from the upstream tube impinges at that point causing rise in the heat transfer at that point. The formation of boundary layer in both the direction from the point of impingement causes a decrease in the heat transfer in both the direction. Also, the formation of minima which marks the shear separation (100-120) ° and (235-255)° is delayed compared to the upstream tube. In this case also the heat transfer from the frontal portion (0-100)° and (240-360)° is more compared to the rear portion (100 to 240) °.

Fig 4(c&d) shows the Nusselt number distribution in CV-ST CR 0.5 SR 2.0 combination. In upstream CV tube, separation of laminar shear layer takes place around (80-115)° and (240-270)°, slight depression at around (140-155)° and (205-215)° is observed due to turbulent shear layer separation. Both the front and the rear potion of the tube contributes towards heat transfer in CV tube while suppression of heat transfer in the wake region of ST tube is observed and most of the heat transfer takes place from frontal portion of the tube (0 to 120)° and (245 to 360)°. Lower z/H has lower contribution in the heat transfer. Fig.4(e&f) shows Nusselt number distribution over CX-ST CR 1.5 SR 1.5 combination. Fig.4e shows that in CX tube heat transferred in the zone (0 to 80) ° and (250 to 360) ° is almost same for all the z/H, however in the zone (80 to 250) °, different z/H transfer has different heat transfer. Except for z/H=0, the heat transfer from the rear zone of the CX tube is much larger than the frontal portion. In general, the rise in heat transfer (in the zone of 80° to 250°) is higher for higher z/H. Higher z/H contributes towards more heat transfer compared to lower z/H. Also, the heat transferred is almost symmetrical about rear stagnation point for higher z/H, i.e., from (0-180)° and (180-360)°. Heat transfer from ST tube is shown in Fig.4f. The heat transfer from the frontal portion (0-120)° and (240-360)° contributes more towards the heat transfer compared to the wake portion of the tube. Maxima formation at around 60° and 300° takes place because of the impingement of the separated shear layer from both side of the upstream tube. The heat transfer is more from the (180-360)° compared to (0-180)° because of interference effect of the tubes.

5.3. Pressure Distribution

The pressure distribution in terms of coefficient of pressure $\{C_P=(P-P_\infty)/0.5\rho U_\infty^2\}$ has been discussed in this section. Figure 5a shows pressure coefficient distribution in the upstream tube of ST-ST combinations. The pressure is maximum at front stagnation point and decrease as the flow accelerates towards the surface of the tube and forms minima in the range of around (55-70)° and (270-290)°, after which a small recovery of pressure takes place and finally flow separation takes place around (70-90)° and (260-240)°. The pressure coefficient then falls till the rear stagnation point for all the spacings expect for SR=1.5 which shows large variation in the wake due to interference effect of other tubes because of small spacing between the tubes.

Edelweiss Applied Science and Technology
ISSN: 2576-8484
Vol. 9, No. 5: 2965-2979, 2025
DOI: 10.55214/25768484.v9i5.7626

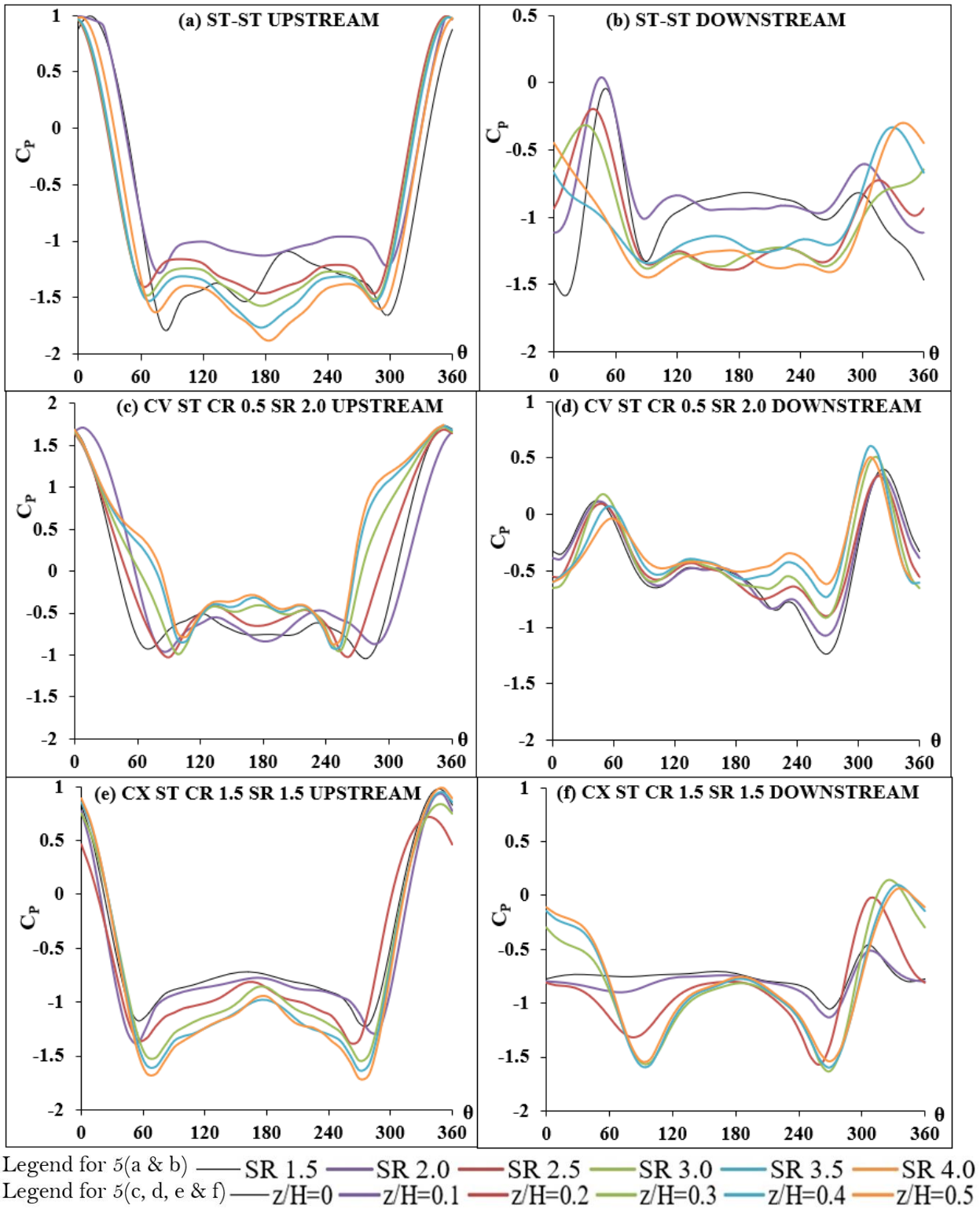

Figure 5.
Pressure coefficient for Number distribution over the surface of the tube at different SR and CR.

Edelweiss Applied Science and Technology
ISSN: 2576-8484
Vol. 9, No. 5: 2965-2979, 2025
DOI: 10.55214/25768484.v9i5.7626

Figure 5b shows that the pressure distribution in the downstream tube of ST-ST combination, the tube has relatively lower variation of pressure compared to that of the upstream tube and suction pressure is dominant in the wake of the upstream tube. For SR=1.5 to 3.0, the pressure distribution has a local maxima formation in the range of (35-55)° because of shear layer attachment from the upstream tube in this range. The attachment angle shift towards the front stagnation point (0°) with increase in SR and vanishes for SR=3.5 and 4.0. This reattachment of shear layer leads to formation of a hump shape. The wake region of the downstream tube remains relatively flat compared to upstream tube which is due to vortex shedding effect in the downstream tube. Also, the pressure variation in the range (270-360)° is lesser compared to (0-90)°. This suppression of pressure is due to interference effects of interacting tubes. Fig. 5(c&d) shows pressure coefficient distribution in CV-ST CR 0.5 SR 2.0. The upstream CV tube has higher pressure compared to ST-ST case and CX-ST case which is discussed below. This may be because the flow pathlines are deflected towards the central location in case of concave tubes. The wake of the CV tube has irregular pressure distribution because of high interference effect of tubes as the CV tube is projected inwards, towards the downward tube and thereby increasing the interference effect of the other tubes. The downstream ST tube has almost same pressure distribution in the (0-180)° for all z/H, however, the shear layer interference in the (180-360)° leads to different pressure distribution for different z/H. Fig.5e shows the distribution of pressure on CX tube in CX-ST CR 1.5 SR 1.5 at different z/H. The pattern of distribution is similar to upstream tube in ST-ST combination; however, the pressure rises from separation point till the rear stagnation point (180°) instead of falling as in case of ST-ST arrangement. The fsp has lower pressure compared to upstream tube in ST-ST case and the flow separation is delayed with increase in z/H. Fig.5f shows pressure coefficient distribution on ST tube in CX-ST CR 1.5 SR 1.5 combination. Negative pressure dominates as it lies in the wake of CX tube which produces vortices. The pressure variation is higher at higher z/H (0.3,0.4 and 0.5).

5.4. Vortex Contours

Vortex core region helps to identify the areas in the flow-structure where vortices or the rotational structures are present. Three-dimensional vortex core region of the CX-ST and CV-ST combination with maximum and minimum possible CR and SR has been shown in the Fig.6. A highly turbulent nature of the vortex core is evident in the wake of the downstream tube of all configuration. The strong vortices produced behind the tubes is responsible for high intermixing of the fluid and hence increase in heat transfer of CT-ST tubes compared to ST-ST tubes.

5.5. Heat Transfer Ratio (HTR)

Heat transfer ratio (HTR) has been defined as the heat transfer from a particular CT-ST configuration to the heat transfer from corresponding ST-ST combination having same SR. Positive HTR signifies that the heat transfer is increased when CT-ST combinations are used and vice-versa for negative HTR. Mathematically,

$$HTR = \frac{HEAT\ TRANSFERED\ BY\ A\ (CT-ST) configuration\ at\ a\ particular\ PR - HEAT\ TRANSFERED\ BY\ THE\ (ST-ST) combination\ at\ the\ same\ PR}{HEAT\ TRANSFERED\ BY\ THE\ (ST-ST) combination\ at\ the\ same\ PR} x100$$

Edelweiss Applied Science and Technology
ISSN: 2576-8484
Vol. 9, No. 5: 2965-2979, 2025
DOI: 10.55214/25768484.v9i5.7626

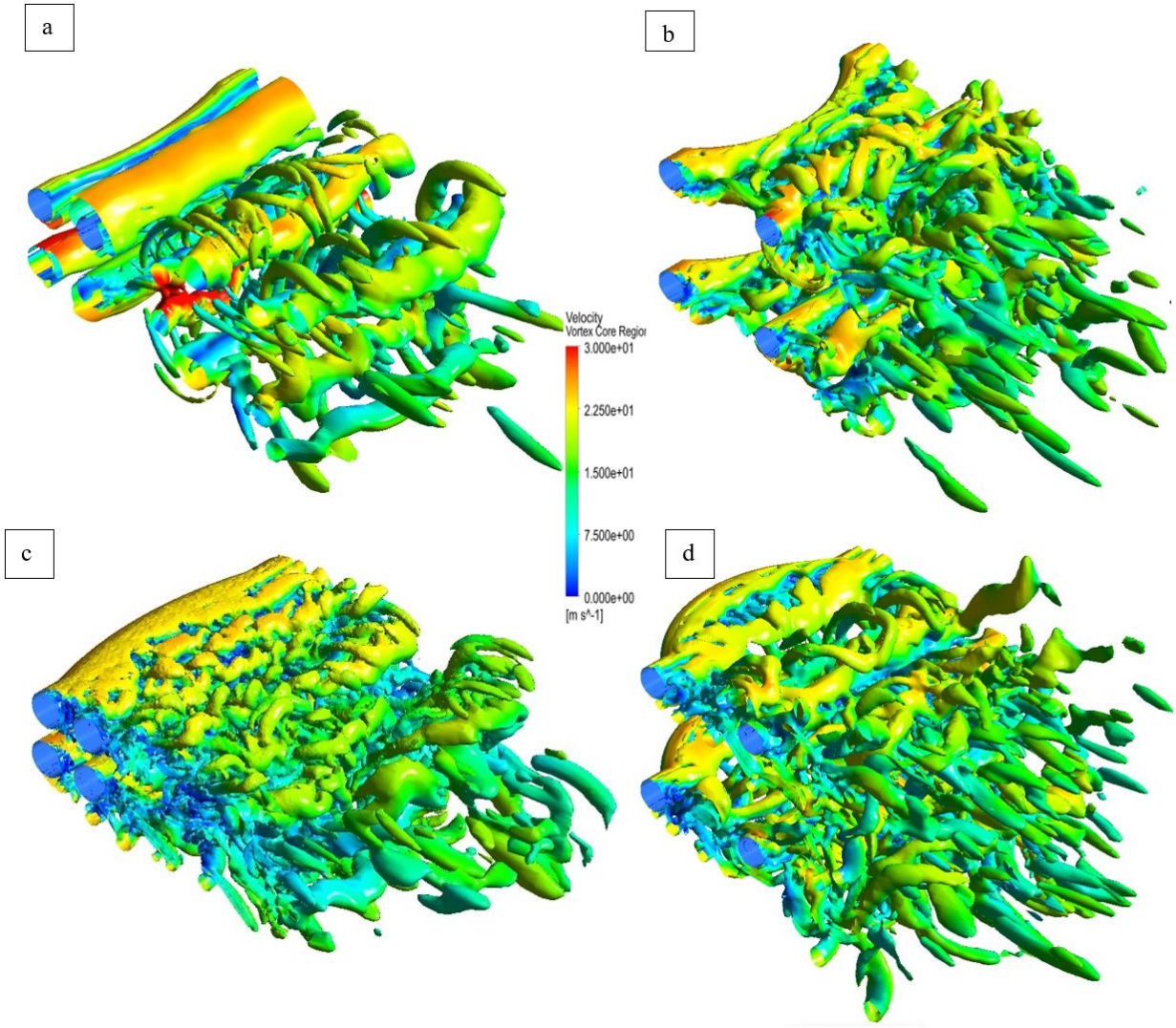

Figure 6.
Normalized velocity magnitude with vortex core region (based on Q* criteria set at 0.01) of a) CX-ST CR 0.5 SR 1.5 b) CX-ST CR 1.5 SR 4.0 c) CV-ST CR 0.5 SR 2.0 d) CV-ST CR 1.5 SR 4.0.

Figure 7 shows the HTR for CX-ST and CV-ST combinations. 16 out 18 of configurations of CX-ST combination shows improved heat transfer compared to corresponding ST-ST combination. A general trend in the CX-ST combination is that HTR increases from SR 1.5 and reaches maximum value at SR 3.0 and then decreases. This may be attributed to change in the flow regime at SR>3.0. Similarly, all the 12 CV-ST combination have higher heat transfer compared to corresponding ST-ST combination. In case of CV-ST combinations also the SR=3.0 corresponds to maximum HTR and beyond SR 3.0, the HTR decreases and minimum HTR is found in the SR=4.0.

Edelweiss Applied Science and Technology
ISSN: 2576-8484
Vol. 9, No. 5: 2965-2979, 2025
DOI: 10.55214/25768484.v9i5.7626

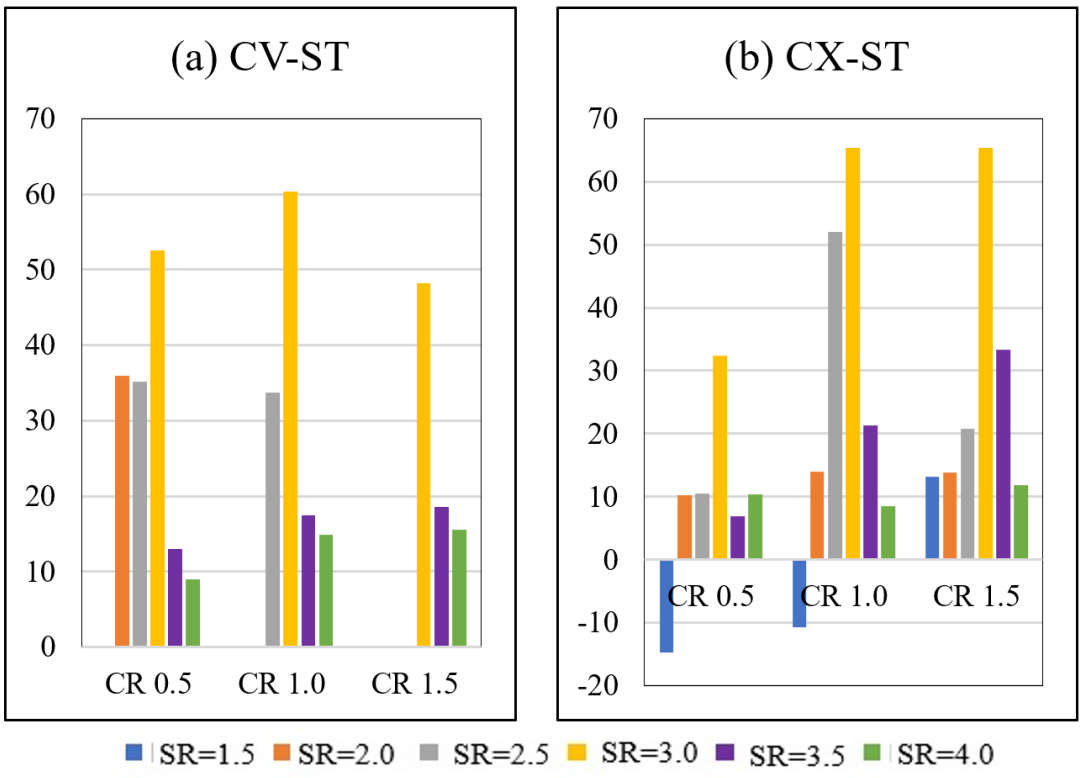

Figure 7.
Heat transfer ratio for different combination of CT-ST tubes.

6. Conclusion

This paper presents a novel configuration of four tubes in square arrangement having curved tubes in upstream position and straight tube in downstream position. The effect of varying the CR of the curved tubes and SR between the tubes on the thermal performance of the tube array have been presented in detail. Based on these study following conclusions may be drawn:

1. The curvature ratio and spacing ratio have considerable influence on the thermal performance of the CT-ST tubes. Amongst all the combination studied, CX-ST CR 1.5 SR 1.5 is having maximum heat transfer.
2. All the 12 possible CV-ST has positive HTR and 16 out of 18 CX-ST combination has positive HTR. This signifies that use of curved tube in the upstream position enhances the heat transfer of the entire array for most of the cases. SR=3.0 is having maximum HTR irrespective of CR for all the CT-ST combinations.
3. The CX-ST CR 1.5 SR 1.5 has the maximum Nu_{avg}. Maximum heat transfer enhancement was found in CX-ST CR 1.5 SR 3.5 with HTR=65.43%. Amongst CV-ST combinations CR 1.0 PR 3.0 gave the maximum HTR=60.38%.
4. The vortex core region of the tubes shows a very turbulent and unsteady flow past the cylinder which helps in the intermixing of the incoming fluid and enhancing the heat transfer.

Acknowledgement:

The authors express their gratitude for the laboratory facility provided by the Department of Mechanical Engineering, Birla Institute of Technology, Mesra, Ranchi, India.

Transparency:

The authors confirm that the manuscript is an honest, accurate, and transparent account of the study; that no vital features of the study have been omitted; and that any discrepancies from the study as planned have been explained. This study followed all ethical practices during writing.

References

[1] A. M. Lavasani and H. Bayat, "Numerical study of pressure drop and heat transfer from circular and cam-shaped tube bank in cross-flow of nanofluid," *Energy Conversion and Management*, vol. 129, pp. 319-328, 2016. https://doi.org/10.1016/j.enconman.2016.10.029

[2] D. Lee, J. Ahn, and S. Shin, "Uneven longitudinal pitch effect on tube bank heat transfer in cross flow," *Applied Thermal Engineering*, vol. 51, no. 1-2, pp. 937-947, 2013. https://doi.org/10.1016/j.applthermaleng.2012.10.031

[3] D. Bacellar, V. Aute, Z. Huang, and R. Radermacher, "Airside friction and heat transfer characteristics for staggered tube bundle in crossflow configuration with diameters from 0.5 mm to 2.0 mm," *International Journal of Heat and Mass Transfer*, vol. 98, pp. 448-454, 2016. https://doi.org/10.1016/j.ijheatmasstransfer.2016.02.072

[4] A. G. Abramov, A. M. Levchenya, E. M. Smirnov, and P. E. Smirnov, "Numerical simulation of liquid metal turbulent heat transfer from an inline tube bundle in cross-flow," *St. Petersburg Polytechnical University Journal: Physics and Mathematics*, vol. 1, no. 4, pp. 356-363, 2015. https://doi.org/10.1016/j.spjpm.2016.02.002

[5] C. K. Mangrulkar, A. S. Dhoble, S. G. Chakrabarty, and U. S. Wankhede, "Experimental and CFD prediction of heat transfer and friction factor characteristics in cross flow tube bank with integral splitter plate," *International Journal of Heat and Mass Transfer*, vol. 104, pp. 964-978, 2017. https://doi.org/10.1016/j.ijheatmasstransfer.2016.09.013

[6] S. Dhiman, A. Kumar, and J. Prasad, "Heat transfer by satellite cluster of cylinders at subcritical Reynolds number," *Heat and Mass Transfer*, vol. 55, pp. 595-612, 2019. https://doi.org/10.1007/s00231-018-2426-z

[7] P. Hishikar, V. K. Gaba, S. K. Dhiman, and A. K. Tiwari, "Heat transfer analysis of nine cylinders arranged inline and staggered at subcritical Reynolds number," *Numerical Heat Transfer, Part A: Applications*, pp. 1-22, 2024. https://doi.org/10.1080/10407782.2024.2363495

[8] J. Du and Y. Hong, "Numerical simulation on fluid flow and heat transfer characteristics in inward sinusoidal rib enhanced tube heat exchangers for waste heat recovery: Comparisons and parametric studies," *International Journal of Thermal Sciences*, vol. 167, p. 107030, 2021. https://doi.org/10.1016/j.ijthermalsci.2021.107030

[9] A. Holfeld, "Experimental investigation of heat transfer and pressure drop in compact waste heat recovery units," Master's Thesis, Technical University of Munich, 2016.

[10] Kunal and S. K. Dhiman, "An experimental study on effect of curvatures of upstream tube on thermal performance of downstream tube in cross-flow of air," *Scientific Reports*, vol. 15, no. 1, p. 14669, 2025. https://doi.org/10.1038/s41598-025-99239-7

[11] A. Haibullina, A. Khairullin, D. Balzamov, V. Ilyin, V. Bronskaya, and L. Khairullina, "Local heat transfer dynamics in the in-line tube bundle under asymmetrical pulsating flow," *Energies*, vol. 15, no. 15, p. 5571, 2022. https://doi.org/10.3390/en15155571

[12] A. Khalatov, G. Kovalenko, and A. Z. Meiris, "Heat transfer in air flow across a single-row bundle of tubes with spiral grooves," *Journal of Engineering Physics and Thermophysics*, vol. 91, pp. 64-71, 2018. https://doi.org/10.1007/s10891-018-1719-x

[13] A. Žukauskas, *Heat transfer from tubes in crossflow* (Advances in heat transfer). Elsevier. https://doi.org/10.1016/S0065-2717(08)70038-8, 1972.

[14] I. Morenko and V. Fedyaev, "Influence of turbulence intensity and turbulence length scale on the drag, lift and heat transfer of a circular cylinder," *China Ocean Engineering*, vol. 31, pp. 357-363, 2017. https://doi.org/10.1007/s13344-017-0042-1

[15] C. Xiao and G. Zhang, "Arrangement effect on heat transfer and hydrodynamic characteristics of a tube bank in cross flow," *Computational Thermal Sciences: An International Journal*, vol. 14, no. 6, pp. 29–51, 2022. https://doi.org/10.1615/ComputThermalScien.2022042191

[16] R. A. Patil, M. R. Nandgaonkar, and C. M. Sewatkar, "On the combined influence of Reynolds number and cylinder spacing for flow around a row of heated square cylinders," *Heat Transfer*, vol. 52, no. 7, pp. 4798-4828, 2023. https://doi.org/10.1002/htj.22908

[17] A. Benmansour and H. Laidoudi, "Evaluation of the effect of rotational speed and rheological nature on heat transfer of complex fluid between two cylinders," *Archives of Thermodynamics*, vol. 45, no. 1, pp. 65–73, 2024. http://dx.doi.org/10.24425/ather.2024.150439

[18] F. Zafar and M. M. Alam, "Flow structure around and heat transfer from cylinders modified from square to circular," *Physics of Fluids*, vol. 31, no. 8, p. 083603, 2019. https://doi.org/10.1063/1.5109693

[19] P. Hishikar, V. K. Gaba, S. Dhiman, and A. K. Tiwari, "Thermal performance of four cylinders in different layouts of spacing ratios under cross-flow at Reynolds number of 35000," *Ocean Engineering*, vol. 281, p. 114834, 2023. https://doi.org/10.1016/j.oceaneng.2023.114834

[20] W. Khan, J. Culham, and M. Yovanovich, "Convection heat transfer from tube banks in crossflow: Analytical approach," *International Journal of Heat and Mass Transfer*, vol. 49, no. 25-26, pp. 4831-4838, 2006. https://doi.org/10.1016/j.ijheatmasstransfer.2006.05.042

[21] N. Aydin, A. Ozalp, and I. Karagoz, "Numerical investigation of heat and flow characteristics in a laminar flow past two tandem cylinders," *Thermal Science*, vol. 25, no. 4 Part A, pp. 2807-2818, 2021. https://doi.org/10.2298/TSCI201119175A

[22] T. Igarashi, "Characteristics of the flow around two circular cylinders arranged in tandem," *Bulletin of JSME*, vol. 24, no. 188, pp. 323-331, 1981. https://doi.org/10.1299/jsme1958.24.323

[23] T. Igarashi, "Characteristics of the flow around two circular cylinders arranged in tandem: 2nd report, unique phenomenon at small spacing," *Bulletin of JSME*, vol. 27, no. 233, pp. 2380-2387, 1984. https://doi.org/10.1299/jsme1958.27.2380

[24] X. Hu, X. Zhang, and Y. You, "On the flow around two circular cylinders in tandem arrangement at high Reynolds numbers," *Ocean Engineering*, vol. 189, p. 106301, 2019. https://doi.org/10.1016/j.oceaneng.2019.106301

[25] X. Wang, K. Gong, H. Liu, J.-X. Zhang, and S. Tan, "Flow around four cylinders arranged in a square configuration," *Journal of Fluids and Structures*, vol. 43, pp. 179-199, 2013. https://doi.org/10.1016/j.jfluidstructs.2013.08.011

[26] C. Liang and G. Papadakis, "Large eddy simulation of cross-flow through a staggered tube bundle at subcritical Reynolds number," *Journal of Fluids and Structures*, vol. 23, no. 8, pp. 1215-1230, 2007. https://doi.org/10.1016/j.jfluidstructs.2007.05.004

[27] S. Benhamadouche and D. Laurence, "LES, coarse LES, and transient RANS comparisons on the flow across a tube bundle," *International Journal of Heat and Fluid Flow*, vol. 24, no. 4, pp. 470-479, 2003. https://doi.org/10.1016/S0142-727X(03)00060-2

[28] S. Dhiman, A. Kumar, and J. Prasad, "Unsteady computation of flow field and convective heat transfer over tandem cylinders at subcritical Reynolds numbers," *Journal of Mechanical Science and Technology*, vol. 31, pp. 1241-1257, 2017. https://doi.org/10.1007/s12206-017-0223-0

[29] N. Hosseini, M. D. Griffith, and J. S. Leontini, "Flow states and transitions in flows past arrays of tandem cylinders," *Journal of Fluid Mechanics*, vol. 910, p. A34, 2021. https://doi.org/10.1017/jfm.2020.975

[30] J. K. Shang, H. A. Stone, and A. Smits, "Flow past finite cylinders of constant curvature," *Journal of Fluid Mechanics*, vol. 837, pp. 896-915, 2018. https://doi.org/10.1017/jfm.2017.884

[31] T. Xu and J. E. Cater, "Numerical simulation of flow past a curved cylinder in uniform and logarithmic flow," *Ships and Offshore Structures*, vol. 12, no. 3, pp. 323-329, 2017. https://doi.org/10.1080/17445302.2016.1139259

[32] F. Jiang, B. Pettersen, and H. I. Andersson, "Influences of upstream extensions on flow around a curved cylinder," *European Journal of Mechanics-B/Fluids*, vol. 67, pp. 79-86, 2018. https://doi.org/10.1016/j.euromechflu.2017.08.006

[33] J. P. Gallardo, H. I. Andersson, and B. Pettersen, "Turbulent wake behind a curved circular cylinder," *Journal of Fluid Mechanics*, vol. 742, pp. 192-229, 2014. https://doi.org/10.1017/jfm.2013.622

[34] F. Jiang, B. Pettersen, and H. I. Andersson, "Turbulent wake behind a concave curved cylinder," *Journal of Fluid Mechanics*, vol. 878, pp. 663-699, 2019. https://doi.org/10.1017/jfm.2019.648

[35] D. K. Walters and D. Cokljat, "A three-equation eddy-viscosity model for Reynolds-averaged Navier–Stokes simulations of transitional flow," *Journal of Turbulence*, vol. 9, no. 7, pp. 1-27, 2008. https://doi.org/10.1115/1.2979230

[36] T. Tsutsui and T. Igarashi, "Heat transfer enhancement of a circular cylinder," *Journal of Heat Transfer*, vol. 128, no. 6, pp. 580–588, 2006. https://doi.org/10.1115/1.2150832

[37] H. Perkins Jr and G. Leppert, "Local heat-transfer coefficients on a uniformly heated cylinder," *International Journal of Heat and Mass Transfer*, vol. 7, no. 2, pp. 143-158, 1964. https://doi.org/10.1016/0017-9310(64)90079-1

[38] F. Hover, H. Tvedt, and M. Triantafyllou, "Vortex-induced vibrations of a cylinder with tripping wires," *Journal of Fluid Mechanics*, vol. 448, pp. 175-195, 2001. https://doi.org/10.1017/S0022112001005985

[39] M. M. Alam, M. Moriya, and H. Sakamoto, "Aerodynamic characteristics of two side-by-side circular cylinders and application of wavelet analysis on the switching phenomenon," *Journal of Fluids and Structures*, vol. 18, no. 3-4, pp. 325-346, 2003. https://doi.org/10.1016/j.jfluidstructs.2003.07.005

[40] A. Bakkhoshnevis, A. R. Mamouri, and M. Khodadadi, "Experimental investigation for wake of the circular cylinder by attaching different number of tripping wires," *Iranian Journal of Mechanical Engineering Transactions of the ISME*, vol. 17, no. 1, pp. 5-25, 2016. https://doi.org/10.1001.1.16059727.2016.17.1.1.6

Edelweiss Applied Science and Technology
ISSN: 2576-8484
Vol. 9, No. 5: 2965-2979, 2025
DOI: 10.55214/25768484.v9i5.7626